Influence of different types of solvent on the effectiveness of nanolime treatments on highly porous mortar substrates

OTERO, Jorge, STARINIERI, Vincenzo <http://orcid.org/0000-0002-7556-0702>, CHAROLA, A.E. and TAGLIERI, Giuliana

Influence of different types of solvent on the effectiveness of nanolime treatments on highly porous mortar substrates

J. Otero[a*], V. Starinieri[a], A. E. Charola[b], G. Taglieri[c]

[a] *Materials and Engineering Research Institute, Sheffield Hallam University, Sheffield, S1 1WB, UK*

[b] *Museum Conservation Institute, Smithsonian Institution, Washington DC, USA*

[c] *Department of Industrial and Information Engineering and Economics, University of L'Aquila, 67100 L'Aquila, Italy.*

* corresponding author: Tel: +44 1142253500; Fax: +44 114 225 3501; jorge.otero.h@gmail.com.

KEYWORDS: Nanolime; Consolidation; Mortar; Solvent; Conservation

Abstract. Historic calcareous structures suffer from weathering processes that result in the loss of some of their original properties. Nanolime products represent an attractive choice for the consolidation of these substrates containing calcite due to their high chemical compatibility with the original structure. The effectiveness of nanolime products has been widely proven for superficial consolidation treatments (e.g. plasters and wall-paintings). However, its consolidation mechanism in highly porous substrates (e.g. limestones or lime mortars) still needs to be fully understood. The aim of this paper is to study the influence of different types of solvent on the effectiveness of nanolime treatments on highly porous lime-mortars. The consolidation effectiveness is investigated by evaluating changes on superficial cohesion, porosity, drilling resistance, water absorption by capillarity, drying rate and aesthetic properties. Results showed that nanolime dispersed in a mixture of isopropanol (50%) and water (50%) yielded slightly better consolidation properties in terms of reduction in porosity, increase in strength and penetration within coarse lime-mortars than nanolime dispersed in other solvents.

1. Introduction

Over time, building materials can undergo decay processes as a result of the action of atmospheric agents which can lead structures to lose their mechanical properties [1]. Consolidant products are used to recover the mechanical properties of the weathered substrate and should be compatible with the substrate [2].

The consolidation of historic calcareous materials still represents nowadays a challenge in the conservation field due to the lack of compatible, effective and durable consolidants for these materials. Silica-based consolidants such as Tetraethyl orthosilicate (TEOS) or Trimethoxymethylsilane (MTMOS) have been widely used in restoration treatments in the past due to their ease of application, initial strength and proven effectiveness in other substrates. However, in the case of calcareous substrates, the lack of chemical compatibility between them and the substrate lead to unsatisfactory long-term effectiveness, which in many cases can lead to unsatisfactory results on limestones and on marble due to the difficulty of bonding a silicate material to calcite [3-6]. An inorganic consolidant, consisting of a colloidal suspension of $Ca(OH)_2$ in water (limewater), was traditionally used due to the total chemical compatibility with the calcitic substrate. However, this treatment presents some important limitations, such as the introduction of large quantities of water (due to the low solubility of $Ca(OH)_2$ in water), the reduced impregnation depth and the very slow rate of the carbonation process, which in many cases lead to unsatisfactory treatments [7, 8]. In recent years, hydroxyapatite, calcium alkoxides or innovative materials based on nanocomposites of ethyl-silicate have also been tested with promising outcomes [9, 10], but further research needs to be undertaken to assess their long-term effectiveness.

Nanoparticles of $Ca(OH)_2$ (nanolimes) were developed and successfully tested for wall-paintings in 2001, overcoming the limitations of the traditional limewater treatment [11]. Nanolimes preserve the same compatibility of the traditional lime-water treatment while presenting superior consolidation properties to limewater due to the increase of lime particles introduced and to the reduced size of the particles. Nanolimes are colloidal alcoholic or hydro-alcoholic dispersions with higher reactivity and particle concentration, which can improve the consolidating action of the traditional limewater technique in terms of higher penetration, strength and reduction of the application time [12, 13]. Nanolimes have emerged as an efficient consolidant for the superficial consolidation of different historic substrates (e.g. wall-paintings, stuccos or plasters) [14] and for the conservation of other cultural heritage materials such as paper [15], canvas [16], bones [17] and wood [18]. However, the results obtained when applied to highly porous substrates are few and controversial [6, 19, 20] and its consolidation mechanism still needs to be fully understood particularly in relation with the penetration of nanoparticles into the highly porous network.

The effectiveness of nanolime in highly porous substrates can be influenced by several factors: i) low concentration nanolime dispersion (e.g. 5 g/L) can reduce the accumulation of the particles at the surface thus helping the penetration of nanoparticles into the pores [12, 21]; ii) repeated applications increase the consolidation effectiveness [12, 22]; iii) high relative humidity environments (>75%RH) enhance the carbonation process [23]; iv) the type of alcoholic solvent influences the rate of carbonation reaction and the formation of different polymorphs of calcium hydroxide [23, 24]; v) the presence of residual water content in the nanolime suspension and a reduced concentration of the nanolime dispersion enhance the carbonation process [24-26]; vi) nanolime particle size can influence the consolidation effectiveness in relation with the substrate pore structure where larger particle size nanolime tends to be deposited mainly in the large sized pores, while smaller particle size nanolime tends to fill both large and small pores equally [27]; vii) nanolime storage conditions after synthesis (T< 5°C, for short periods of time) reduce the conversion of $Ca(OH)_2$ into Ca-alkoxides which enhances the carbonation process [28].

Nanolimes are applied in a wide range of solvents (i.e. ethanol, propanol, butanol, water or a mixture of these solvents) [12, 29-33]. In recent years, a series of studies suggested that the type of solvent could be critical for the nanolime effectiveness in highly porous substrates [29, 30, 34]. These researches suggested that the deposition of $Ca(OH)_2$ nanoparticles in the pores occurs during the solvent evaporation phase where most of the nanoparticles could migrate back to surface [34]. The same authors also suggested that solvents with low evaporation rate (e.g. water) could be more suitable for coarse porous substrates as they seem to reduce the back-migration of the nanoparticles to the surface contributing to their deposition in-depth [29, 30].

The aim of this paper is to study the influence of different types of solvent on the effectiveness of nanolime treatments on highly porous lime-mortars. In this experimental work, the $Ca(OH)_2$ nanoparticles were dispersed in five solvents at the same concentration (5 g/L) following the same synthesis route and conditions. The consolidation effectiveness of the resulting nanolime treatments was investigated by assessing changes in porosity, superficial cohesion, drilling resistance, water absorption by capillarity, drying rate and aesthetic properties.

2. Materials and methods

2.1 Lime mortar samples

Mortar samples were manufactured from lime powder (Singleton Birch Ultralime CL90) and a fine silica sand (Pentney, UK) in a proportion of 1:2.5 (bulk volume) measured (constant flow of 16 cm) according to the European Standard BS EN 1015-3:1999 [35]. The water:binder ratio to obtain the desired flow was 1.56. Mortars were batched by weight after measuring lime and sand densities according to EN 1015-2:1998 [36]. Mortars were produced by mixing the dry ingredients with water in a Hobart mixer. The mix protocol was as follows: 1) dry mix sand and lime for 2 min at 62 rpm; 2) add water while continuing mixing at 62 rpm for 30 s; 3) stop the mixer for 30 s and scrape the mixer bowl; 4) mix for 5 min at 125 rpm. Samples were cast in 40 x 40 x 160 mm steel moulds in two layers and vibration-compacted. Immediately upon floating off the fresh mortar, the moulds were transferred to a temperature and humidity controlled room maintained at 20 ˚C and 65% RH. Mortar beams were cured at 5-15˚C and 60-80%RH for 28 days under monitored outdoor conditions. Upon completion of the curing period, each prism was cut into 4 cubes measuring approximately 40x40x40 mm which were cured for further 28 days in the same conditions.

The mortar's chemical composition was obtained by X-Ray Fluorescence (*Philips PW2400*). XRF samples consisted of pressed powder pellets (Retsch PP-40 pellet press) and the elemental weight percentages calculated from total oxide X-Ray analysis. XRF results shows that the lime mortar is composed by Si (63.8±0.5%), Ca (32.7±0.1%) and traces of Al (1.2±0.3%), K (1.0±0.3%) and P (0.8±0.3%).

The mortar's mineralogical composition was obtained by X-Ray Diffraction (PANalytical XPert PRO) recorded with a step size of 0.026˚2θ in the angular range 20-70°2θ. X-ray data were fitted using the pseudo-Voigt profile function and refined by means of Rietveld refinement [37, 38]. XRD samples were ground and sieved (80 µm sieve mesh) and placed over an XRD zero-background sample holder prior to the XRD analysis. The XRD-Rietveld refinements show the mortar is composed of 79.9% Quartz (SiO_2, ICSD #00-046-1045) and 20.1% calcite ($CaCO_3$, ICSD #00-005-0586). XRD was not able to identify the presence of any other mineral phases (e.g. feldspar containing Al, K and P, which were elements detected by XRF) suggesting that any other mineral phases containing those elements could be present in amorphous or poorly crystallised phases or in amounts below the instrument detection level (< 1%).

The mortar's pore structure was determined by Mercury Intrusion Porosimetry (MIP) using a *PASCAL 140/240* instrument. The samples for MIP consisted of two mortar fragments measuring approximately 8 x 8 x 15 mm taken from the surface (up to a depth of 20 mm) of the sample, which were dried in an oven at 60 ºC until constant weight. The average porosity of the mortar measured by MIP was 23±1.6 vol.% with a bulk density of 1.698±0.1 g/cm^3.

2.2 Synthesis and characterisation of nanolime

Nanolime was synthesized through a patented process based on an ion exchange process between an anion exchange resin (Dowex Monosphere 550A OH by Dow Chemical) and an aqueous calcium chloride solution ($CaCl_2$ by Sigma-Aldrich), as described in the literature [39, 40, 41]. Following the synthesis, the newly synthetized nanoparticles of $Ca(OH)_2$ were dispersed in five solvents at the same concentration (5 g/L): Isopropanol (IP), Ethanol (ET), Water (W), 50-50% Water-Isopropanol (WIP) and 50-50% Water-Ethanol (WET). A small residual water (W = 5%) was left intentionally in the suspension of IP and ET, as this practice enhances the carbonation process [26, 42]. The relevant properties of the solvents are reported in Table 1. Suspensions were kept in a refrigerator (T < 5 °C) prior the application to minimize the $Ca(OH)_2$ particles conversion into Ca alkoxides [28, 43].

Table 1. Physical-chemical properties of the selected nanolimes

Code	Solvent	g/L	Boiling point (°C)	Surface tension (solvent/air) (N/m)	Treated Samples
IP	Isopropanol	5	82.6	0.0230	3
ET	Ethanol	5	78.3	0.0221	3
W	Water	5	99.6	0.0728	3
WIP	50-50% Water-Isopropanol	5	87.3	0.0247	3
WET	50-50% Water-Ethanol	5	92.2	0.0281	3

The size and shape of the synthetized nanolime particles was determined by TEM (Philips CM200) while their crystalline phases were analysed by XRD (PANalytical X'PertPRO). Both TEM and XRD were carried out immediately after the synthesis and samples were prepared in nitrogen atmosphere (99.99% nitrogen gas) TEM samples were prepared by placing a few drops of the primary nanolime suspension (W) on a TEM carbon-coated

copper grid while XRD samples were prepared by dispersing 0.12 ml of each suspension in an XRD silica sample holder.

The relative kinetic stability (KS) of the suspensions was determined from the variation over time (2 hours) of their absorbance (at λ = 600 nm) using a UV/VIS Spectrophotometer (UV-VIS Spectrophotometer Varian 50SCAN). Nanolimes were agitated before the test to increase their colloidal stability [12]. The KS % was calculated using the following formula:

$$KS\ \% = 1 - [(A_0 - A_t)/A_0] \times 100$$

where A_0 is the starting absorbance and A_t the absorbance at time t, both at a wavelength of 600 nm as described in literature [12, 43].

The surface tension of the solutions was determined by the pendant drop method using an OCA 15 Plus instrument (Dataphysics). For this test, a solution drop (5 µL) was pendant through a Hamilton 50 µL DS 500/GT syringe. The surface tension of the nanolime was calculated by measuring the shape of the pendant drop of the dosing needle, defined with the Young–Laplace equation:

$$AP = \gamma \left(\frac{1}{R1} + \frac{1}{R2} \right)$$

where ‘‘ΔP’’ is the difference in pressure across the interface, ‘‘γ’’ the surface tension, and ‘‘R1’’ and ‘‘R2’’are the curvature radius [44].

2.3 Nanolime carbonation study

The influence of the solvent in the carbonation process was investigated by XRD. Samples were prepared by exposing 0.12 ml of each suspension to outdoor conditions (T ≈ 5-15˚C, R.H ≈ 60-80%) for 1 hour and for 7 days. XRD data was recorded with a step size of 0.026˚2θ in the angular range 15-70°2θ and data were fitted and refined as described in section 2.1.

2.4 Nanolime treatments

160 The treatments were carried out by brush in outdoor conditions (T ≈ 5-15˚C, R.H ≈ 60-80%) in a protocol applied
161 in previous studies [12, 27, 44]. Treatment started two days after the synthesis to reduce the conversion of $Ca(OH)_2$
162 into Ca-alkoxides and improve their effectiveness [28]. Each nanolime (IP, ET, W, WIP and WET) was agitated
163 before each brushstroke and applied on the top face (as cast) surface of three mortar cubes (40 x 40 x 40 mm) per
164 each nanolime. The application was stopped when no absorption was observed (samples reached constant weight
165 and the surface remained completely wet without absorption for a period of at least 1 minute). After saturation, the
166 samples were left to dry and retreated again after 48 hours, when samples were completely dry. Samples were
167 weighed before and after each application (dry weight and saturated weight) to measure the amount of nanolime
168 absorbed by each mortar cube during each application. The treatment was terminated when each cube absorbed 500
169 mg of calcium hydroxide (approximately 100ml) which required approximately 40 days (20 days of nanolime
170 application). Following the treatment, the samples were cured at RH ≈ 60-80%RH under controlled outdoor
171 conditions for 28 days prior to the analysis. A set of Control samples (CO) were kept in the same controlled
172 outdoor conditions for the same period.

173

174 *2.5 Treatment drying rate*

175 The drying rate of the treatments was evaluated by measuring the weight loss over time after saturation of three
176 treated samples per each suspension, in accordance with the EN Standard [45]. The aim of this test is to determine
177 the evaporation rate of each nanolime suspension in order to investigate possible correlations of the solvent
178 evaporation rate with the consolidation effectiveness, as suggested by previous authors [30]. This test was carried
179 out under controlled outdoor conditions (T ≈ 5-15˚C, R.H ≈ 60-80%).

180

181 *2.6 Consolidation effectiveness*

182 Following curing, the consolidation effectiveness was analysed by means of the following techniques and methods.
183 MIP was carried out to measure the influence of the treatments on open porosity and pore size distribution.
184 Samples for MIP were taken from the mortar's surface (up to a depth of 50 mm) of both treated and control
185 samples.

186

Water absorption coefficient (WAC) was measured according to EN 13755 [46]. Upon completion of this test, the samples were totally immersed in water for 24 hours at room atmosphere and the drying behaviour of the samples was also measured [47]. Three cubes per treatment were tested for both treated and control samples.

'Scotch Tape Test' (STT), according to ASTM 2009 [48], was carried out to measure the influence of the treatments on surface cohesion. Nine measures per treatment were obtained for both treated and control samples.

Drilling Resistance Measurement System (DRMS) (SINT-Technology) was carried out to obtain the depth of penetration of each nanolime and their influence on strength. The DRMS was specifically designed for assessing the penetration and effectiveness of consolidants in homogeneous substrates [20]. DRMS tests were carried out using a new drill bit of 5 mm diameter per each sample, rotation speed of 200 rpm, penetration rate 15 mm/min and penetration depth of 20 mm. Six measurements were performed for both control and treated samples and their mean curve was calculated for comparison.

Scanning Electron Microscope (SEM, NanoSEM 450) was used to observe the surface of both treated and control samples. Samples for SEM were coated with a 20nm thick layer of gold using a Quorum Q150T. SEM images were obtained with an ETD detector, a working distance of 3mm, an accelerating voltage of 15 kV and a spot size of 30 nm.

Colorimetric analysis (Minolta CM508D Colorimeter) was undertaken to determine any possible surface colour changes induced by the nanolime treatments. Previous researches reported a whitening appearance after nanolime treatments [12, 32] and this research aims to observe differences regarding the type of solvent used. Thirty measurements were obtained for each control and treated samples, which were taken on random areas of the sample surfaces. Total colour variation (ΔE) was calculated by the formula:

$$\Delta E^{*} = \sqrt{\Delta L^{*2} + \Delta a^{*2} + \Delta b^{*2}}$$

where ΔL* is the change in lightness (white-black parameter), Δa* (red-green parameters) and Δb* (blue-yellow parameters).

3. Results and Discussions

3.1 Characterization of the nanolime suspensions

The TEM photomicrograph in Fig. 1 shows a plate-like hexagonal $Ca(OH)_2$ nanoparticle. This morphology is identical to that observed for nanolime particles analysed in previous studies, which we also synthetized by anion exchange processes [12, 32]. These $Ca(OH)_2$ nanoparticles are regularly shaped and have diameters ranging from 20 to 80 nm, which is also in line with previous research on the same type of nanolime [16, 31, 32].

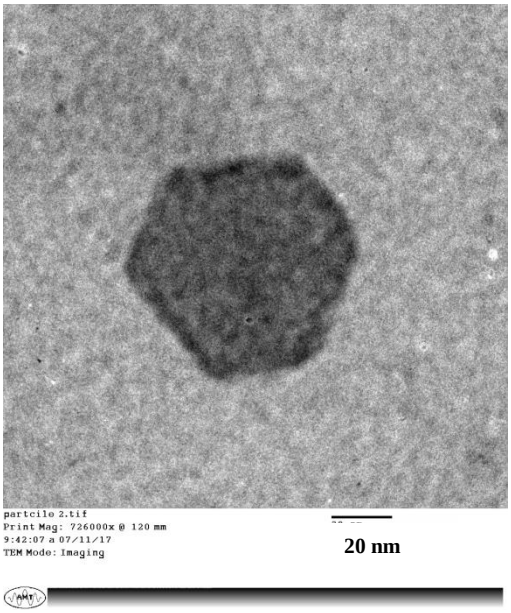

a)

Figure 1. TEM micrograph of a small single particle of synthesised nanolime (IP)

XRD analysis of samples dried in nitrogen atmosphere (Fig.2) show that the only crystal phase present in all suspensions corresponds to Portlandite ($Ca(OH)_2$, ICSD #01-087-0674) except for the W sample (nanolime in water) which contains an approximately 20% amount of calcite (ICSD #01-072-1652). This is attributed to the higher reactivity of the $Ca(OH)_2$ nanoparticles with CO_2 when dispersed in water, as moisture significantly contributes to the carbonation process [26, 31, 33]. Rietveld refinement showed that the W sample consists of 79.3% Portlandite and 20.7% Calcite. For all samples, the strongest peak corresponds to the {001} basal plane. IP, ET, WIP and WEP dry particles have a preferred orientation to the planes {010} or {100}, which are both side planes. The Rietveld refinement factors are included in Table 2.

Table 2. Rietveld refinement factors of samples dried in Nitrogen atmosphere

	Nitrogen				
	IP	ET	W	WIP	WET
R-expected	10.1	9.3	13.1	18.4	13.8
R-profile	11.6	7.9	14.5	15.4	11.7
Weighed R profile	14.6	10.3	12.7	11.1	16.1
Goodness of fit	3.4	3.3	4	4.1	4.3
Phase proportions	100% P	100% P	79.3%P 20.7%C	100% P	100% P
Direction of preferred orientations	010	100	NPO	010	100

NPO (No preferred orientation), P (Portlandite); C Calcite)

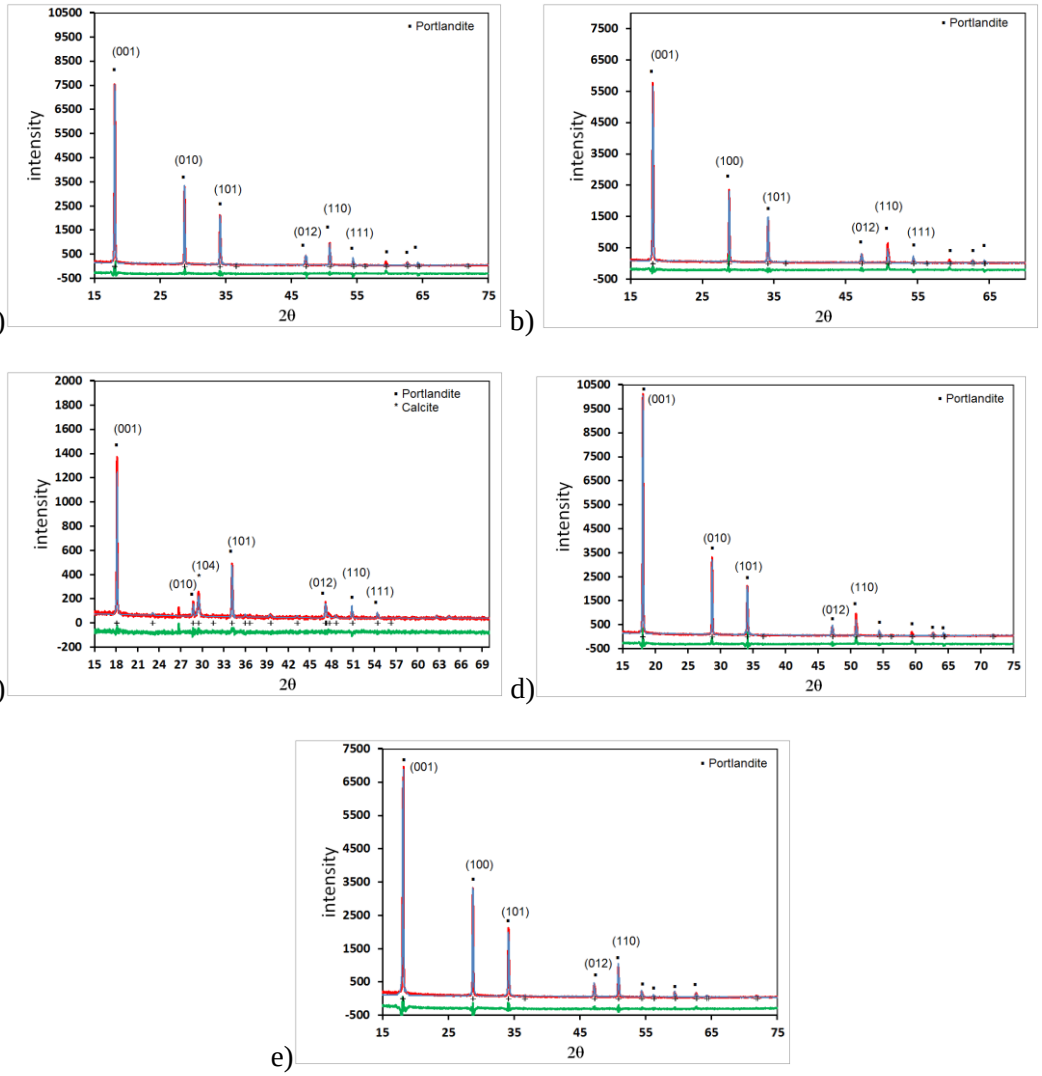

Figure 2. XRD patterns of samples dried under nitrogen atmosphere for; a) IP (Isopropanol); b) E (ethanol); c) W (water); d) WIP (50% Water and 50% Isopropanol); and e) WET (50% water and 50% Ethanol). Red line corresponds to Intensity observed, blue line to Intensity calculated and green line to the Intensity observed - Intensity calculated difference curve. The crystal phases are shown in brackets and the "+" symbol corresponds to the main peaks. In parentheses, the Bragg peaks indexes of portlandite.

Figure 3 shows the colloidal stability of IP, ET, W, WIP and WET suspensions over a period of 2 hours following a moderate agitation. WIP presented the highest colloidal stability (settling speed ≈ 5% per h). Similar results were observed in previous studies carried out on this type of nanolime suspension [12, 31, 32]. The colloidal stability of alcoholic nanolime dispersions synthesised by anionic exchange process is lower than that of nanoparticles synthesised by other routes (e.g. solvothermal reactions or drop-to-drop method), where nanoparticles remain in colloidal state for more than one week [11, 18, 29]. Nevertheless, all dispersions showed a reasonable colloidal stability where most of the nanoparticles (>95%) remain in colloidal state during the first 5-10 minutes after agitation, which is considered acceptable in terms of practical purposes [12].

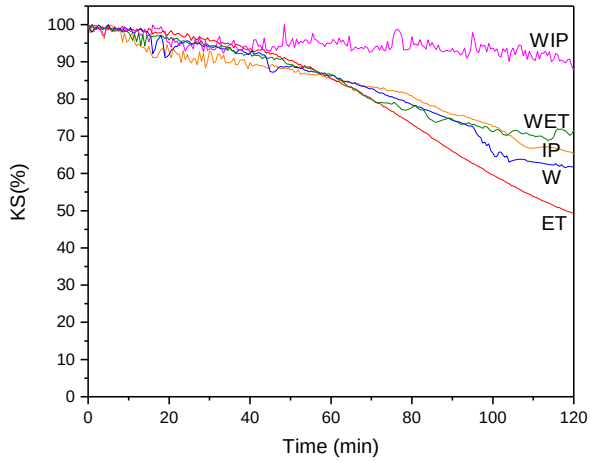

Figure 3. Kinetic stability KS (%) of IP (Isopropanol), E (ethanol), W (water), WIP (50% Water and 50% Isopropanol) and WET (50% water and 50% Ethanol) samples

3.2 Nanolime carbonation study

The XRD analysis of the nanolime suspensions exposed to air for 1 hour (60-80% RH) proved the high reactivity of the nanoparticles (Fig. 4), independently from the solvent. Calcite (ICSD # 01-085-1108) is the only crystalline phase detected for all suspensions. W sample (Water) showed a better developed crystalline structure (Fig. 4c) which confirms the higher reactivity of the $Ca(OH)_2$ nanoparticles when suspended in water. The Rietveld refinement factors are included in Table 3.

Table 3. Rietveld refinement factors of samples exposed to air in outdoor conditions (60-80%RH) for 1h and 7 days.

	1 hour in air	7 days in air

	IP	ET	W	WIP	WET	IP	ET	W	WIP	WET
R-expected	15.8	15.2	14.7	14.7	14.9	15.7	15.3	21.2	15.6	14.8
R-profile	11.3	10.7	12.3	11.4	9.9	11.1	11.3	16.1	16.3	10.8
Weighed R profile	14.3	13.6	16.2	14.5	12.7	14.1	14.1	20.8	20.8	13.7
Goodness of fit	1.8	1.8	1.2	1.9	1.7	1.8	1.8	1.9	1.7	1.8
Phase proportions	100% C	100% C	100% C	100% C	100% C	100% C	100% C	100% C	100% C	100% C
Direction of preferred orientations	NPO	NPO	NPO	NPO	NPO	104	104	104	104	104

NPO (No preferred orientation), P (Portlandite); C (Calcite)

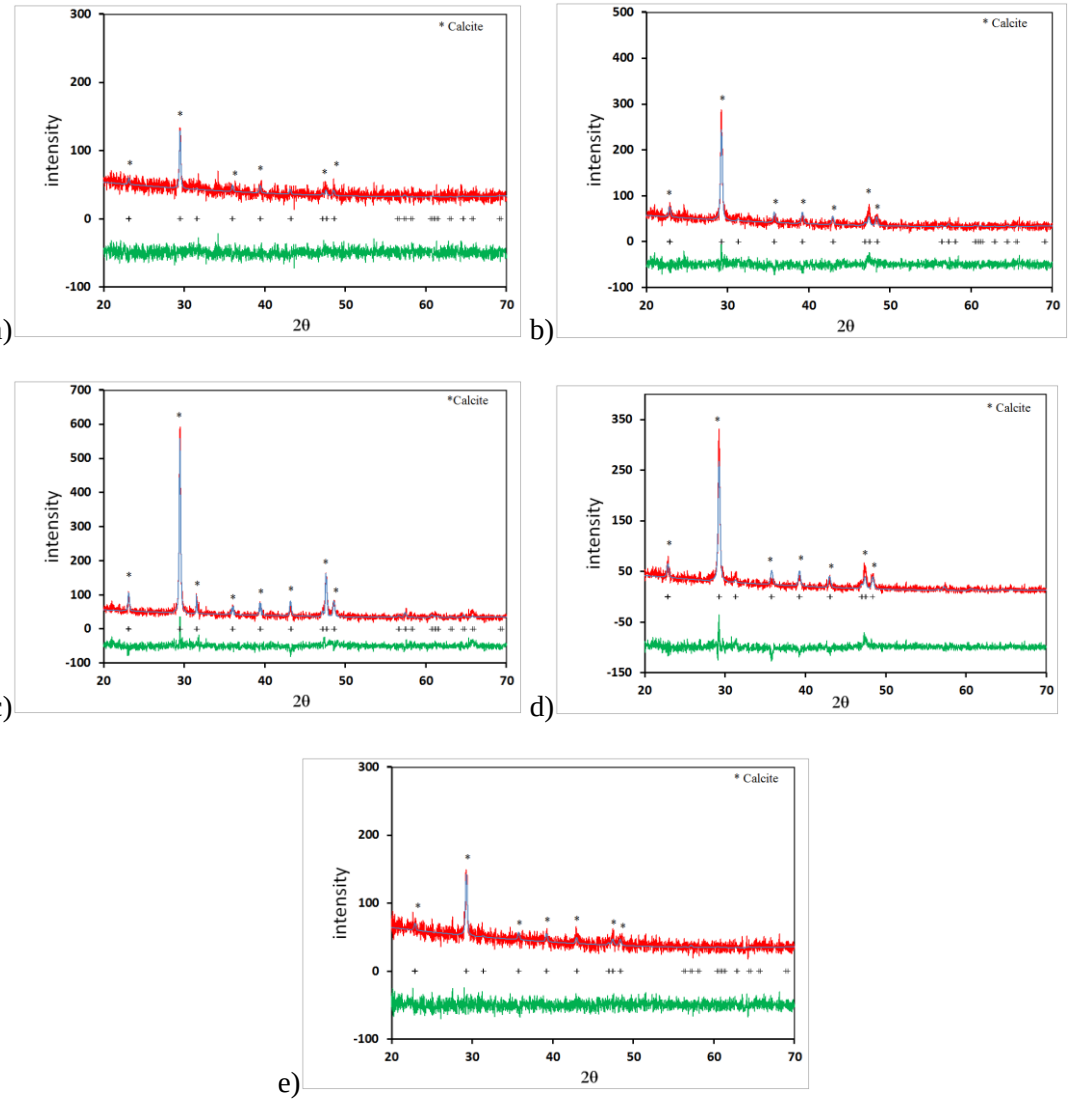

Figure 4. XRD patterns after 1 hour of air exposure (60-80%RH) for; a) IP (Isopropanol); b) E (ethanol); c) W (water); d) WIP (50% Water and 50% Isopropanol); and e) WET (50% water and 50% Ethanol). Red line corresponds to Intensity observed, blue line to Intensity calculated and green line to the Intensity observed - Intensity calculated difference curve. The crystal phases are shown in brackets and the "+" symbol corresponds to the main peaks.

The XRD results after 7 days of air exposure (Fig. 5) show that all samples are composed of pure calcite crystals ($CaCO_3$, ICSD# 01-086-2334) oriented to {104}, similar to that reported in previous studies [12, 31]. The low intensity recorded for the IP (Isopropanol) sample (Fig. 5a) suggests this sample presents a slightly poorer crystalline phase. The Rietveld refinement factors are included in Table 3.

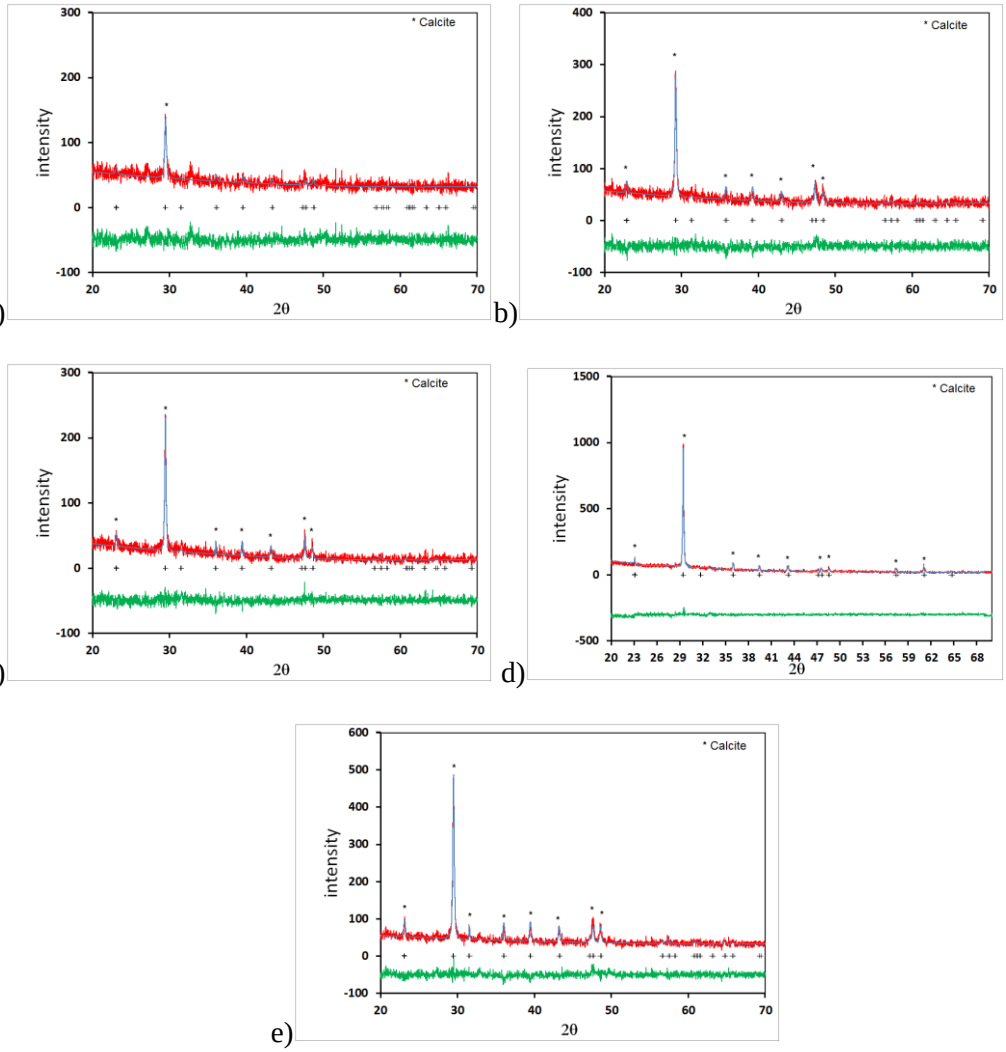

Figure 5. XRD patterns after 7 days of air exposure (60-80%RH) for; a) IP (Isopropanol); b) E (ethanol); c) W (water); d) WIP (50% water and 50% Isopropanol); and e) WET (50% water and 50% Ethanol). Red line corresponds to Intensity observed, blue line to Intensity calculated and green line to the Intensity observed - Intensity calculated difference curve. The crystal phases are shown in brackets and the "+" symbol corresponds to the main peaks.

3.3 Treatment drying rate

Figure 6 shows the evaporation kinetics of the nanolimes after their application. ET and IP treatments evaporated faster compared to the other treatments, which can be attributed to the lower boiling point of ethanol and

isopropanol (Table 1). Both solvents completely evaporated in approximately 24 hours. In contrast, WIP and WET treatments required approximately 28 hours. This could be attributed to the fact that both isopropanol and ethanol form azeotropic mixtures with water (87,7% and 95.4% alcohol respectively) with the latter having a lower boiling point (78.4ºC) than the isopropanol one (82.6ºC). The W sample took some 48 hours to dry. The evaporation of W treatment is slower due to the higher surface tension of water that enhances its retention within the pore network, delaying the drying rate [30, 49].

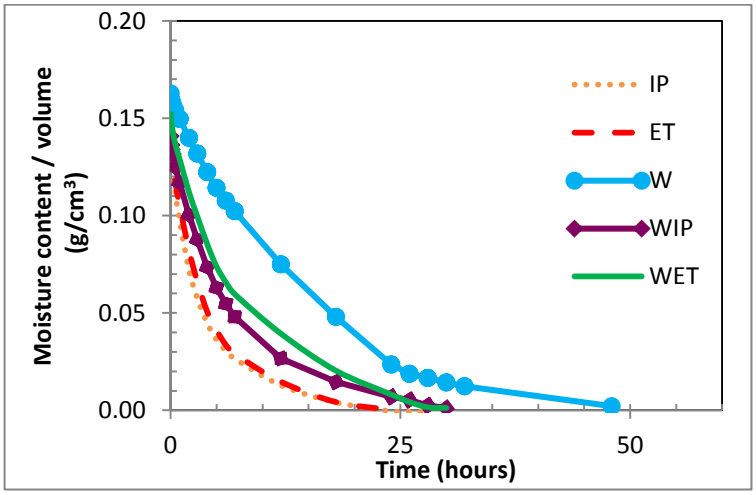

Figure 6. Drying kinetic curves for the treated mortars

3.4 Consolidation effectiveness

The porosity and pore structure properties of the control and treated mortars are summarised in Table 4. All treatments caused a slight reduction in the porosity of the mortar near the surface (samples taken within 50 mm from the surface), apart from IP sample where the standard deviation makes this difference statistically insignificant. WIP yielded a slightly higher reduction in porosity (23% reduction), followed by W (17%), compared to the other treatments (from 6 to 12%). All samples showed an increased total pore surface area (m^2/g), suggesting the presence of a higher amount of smaller pores after treatment, as confirmed from the MIP curves (Fig. 7).

Table 4. Porosity properties of treated and untreated samples. CO*: control sample, numbers in brackets are the standard deviation

	Porosity (vol.%)	**Total pore surface area (m^2/g)**
CO*	23.34 (±0.34)	0.674 (±0.28)
IP	22.82 (±0.40)	1.955 (±0.41)

ET	21.85 (±0.51)	1.227 (±0.45)
W	19.36 (±0.38)	1.393 (±0.36)
WIP	17.87 (±0.71)	1.328 (±0.51)
WET	20.38 (±0.09)	1.29 (±0.21)

The MIP curves show that the porosity reduction in the samples treated with WIP and WET (Fig. 7d and 7e respectively) can be attributed mainly to the reduction in the population of pores with larger diameter (17 to 100 µm). The reduction in larger pores in both samples is also accompanied by an increase of the intermediate pores (diameters 1 to 10 µm). This effect is also observed for the sample treated with IP (Fig. 7a) although this sample presents no visible reduction of the pores with larger diameter size (17 to 100 µm). In contrast, IP and W nanolimes seem to be more effective in filling the pores with smaller size (0.05 to 0.7 µm), defining a new pores population of diameter < 0.050 µm. These results suggest that nanolime in a water-alcohol solution tends to be more effective in filling the larger pores than nanolime in alcohols only or in water only which, in contrast, favour an increase of the surface area thanks to the presence of micropores, in accordance with previous results obtained from aqueous nanolime suspension [33].

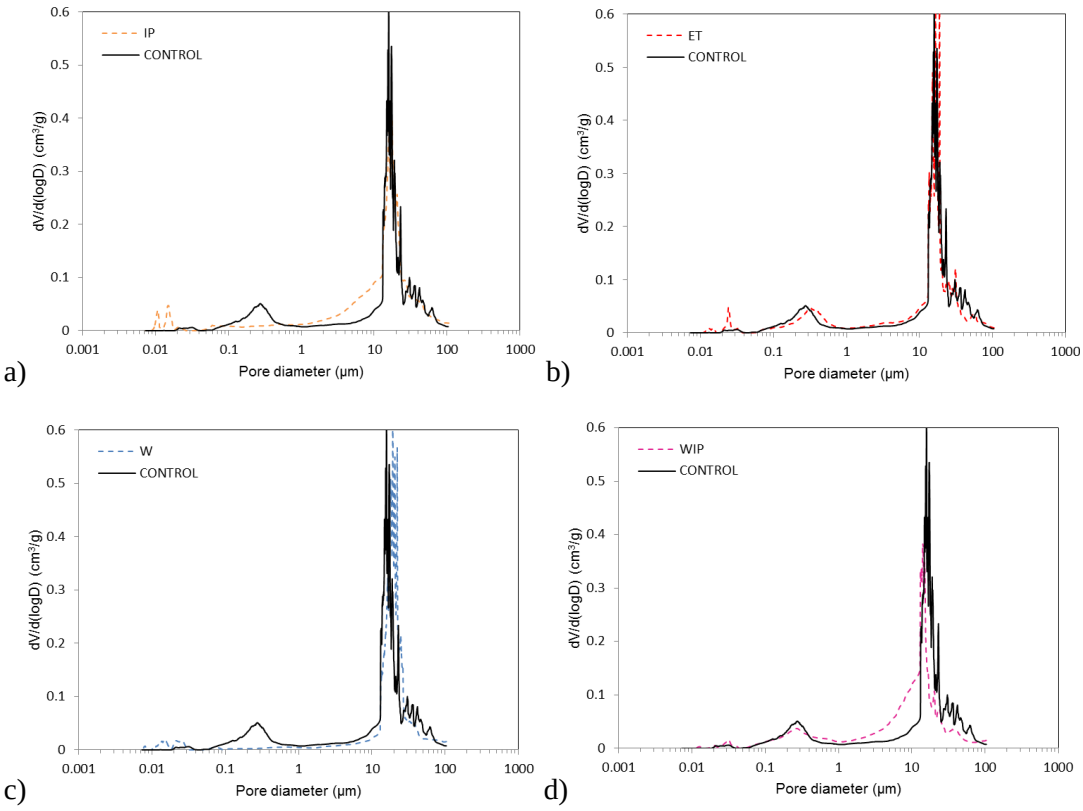

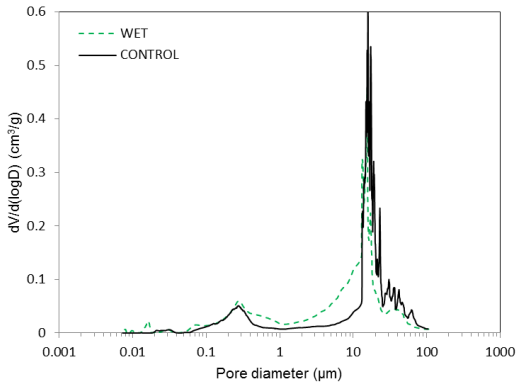

e)

Figure 7. Pore size distribution of control and treated samples: a) IP; b) ET; c) W; d) WIP; and e) WET.

The water absorption and drying curves are reported in Fig. 8 and Fig. 9, and water absorption and drying characteristics are reported in Table 5. The denser pore structure at the surface slightly affected the water absorption and drying kinetics of the samples. Results show that all treatments slightly delayed the water absorption by capillary compared to control samples (Fig 8). WIP and W seem to present the higher reduction of the water absorption by capillary curves than the other treatments. All treated samples also presented a decrease of the water absorption coefficient (WAC), although the high standard deviation makes this decrease not statistically significant (Table 5). This decrease of the water absorption by capillary is due to a reduction of the porosity at the mortar's outer 1cm (MIP and DRMS analysis), which slows down the capillary rise [49]. WIP and W samples required more time (30 minutes more) to reach the asymptotic values than the other treatments (Fig. 8). All treated samples also presented a decrease of the water absorbed at asymptotic value (Table 5), although the standard deviation also indicates that the decrease is not statistically significant. These results could be in accordance to the MIP results reported above which suggest that WIP and W treatments yielded higher reduction on porosity.

Table 5. Apparent porosity by immersion, water absorption and drying characteristics

Parameter	**CO**	**IP**	**ET**	**W**	**WIP**	**WET**
Capillary absorption coefficient (10^{-3}g/cm^2 s$^{0.5}$)	17,1 (± 2.74)	15,8 (±2.46)	13,7 (±2.24)	13,2 (±3.18)	12,1 (±2.28)	15,2 (±2.22)
Water absorbed at asymptotic value (g)	11.05 (± 0.49)	10.9 (±0.25)	10.85 (± 0.10)	10.36 (±0.40)	10.56 (± 0.56)	10.55 (± 0.53)
Initial drying rate (10^{-3}g/ cm^3 h)	4,3 (±0.3)	3,6 (±0. 3)	3,5 (±0. 2)	3,2 (±0. 2)	2,7 (±0. 2)	2,6 (±0. 2)
Time for total drying (h)	± 60	± 70	± 78	± 78	± 78	± 78

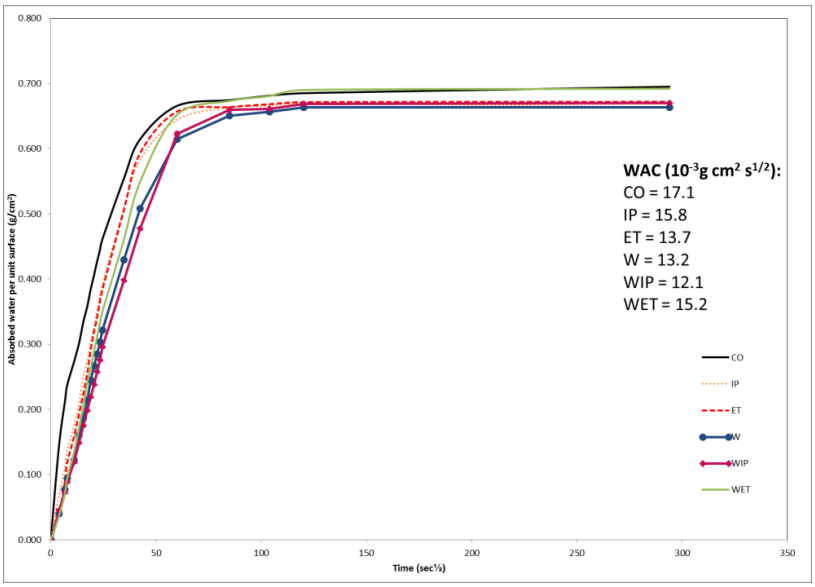

Figure 8. Capillary absorption curves of treated specimens (solvents).

The drying kinetics curves and the initial and final drying rates are shown in Fig. 9 and Table 5. Results showed that all treatments slowed the initial drying rate of the specimens, which was also noticed in previous work [12, 27, 44]. This was attributed to the denser pore structure in the specimens' surface, which reduces the water transport towards the surface slowing down the drying [12]. Control samples were completely dry after 60 hours. In contrast, IP samples needed approximately 70 hours to dry while ET, W, WIP and WET samples needed more than 75 hours.

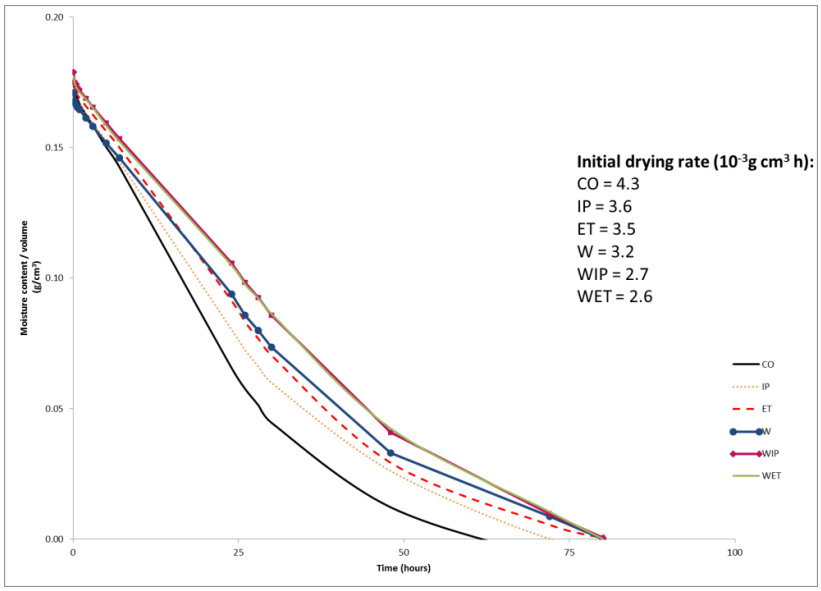

Figure 9. Drying curves of treated specimens (solvents).

355

356 The results of the Scotch Tape Test (STT) are shown in Table 6. All treatments resulted in a similar decrease of
357 removed material ($\Delta W \approx 80\%$). These results confirm that the surfaces of all treated samples improved surface
358 cohesion after nanolime treatments, regardless of the nanolime used.

359

Table 6. Scotch Tape Test (STT): experimental results

Code ID	Released material (mg/cm^2)	ΔW (%)	SD
CO	67.65	-	18.3
IP	9.42	86.1	3.6
ET	7.72	88.6	4.8
W	16.19	80.2	9.4
WIP	12.64	81.3	8.1
WET	15.8	80.9	6.2

Scotch area: 3 x 1.5 cm; SD (Standard Deviation) of released material

360

361

362 Drilling resistance results are shown in Figure 10. The control samples presented a constant drilling resistance (F ~
363 0N (±0.12)) throughout the drilling depth (20 mm). Results show that IP, ET, W and WET treatments clearly
364 increase the drilling resistance of the mortar within about 2-3 mm from the surface more than an order of
365 magnitude (up to a resistance of 1.5N). Additionally, a small consolidation effect (drilling resistance increased to F
366 ~ 0.35N) is also noticeable up to a depth of 10 mm for these samples. The W sample yielded the highest increase in
367 the drilling resistance in the outer 2-3 mm (>1.5 N). This is attributed to the high reactivity of the nanoparticles and
368 the low kinetic stability of this suspension, which could facilitate the accumulation and carbonation of the
369 nanoparticles on the surface. In contrast, the consolidation effect of WIP, which was found as the most stable
370 nanolime suspension (Fig. 3), appears to be more homogeneous within a depth of 6-7 mm (Fig. 10d). This would
371 be preferable as it does not result in the formation of a thin superficial layer which could increase the risk of
372 spalling due to processes such as freeze-thaw or salt crystallization occurring beneath this layer. However, further
373 research must be carried out to fully understand the penetration of these treatments.

374

375 Recent studies carried out by Borsoi et. al. [29, 30, 34] concluded that nanolime deposition in the pores can be
376 influenced by the type of solvent. These researches concluded that nanoparticles tend to migrate back to the surface
377 during the evaporation of the solvent, thus solvents with slower evaporation rate can enhance the deposition of

nanoparticles in the pores in highly porous substrates. In the present study, DRMS results show that there is not a clear correlation between the evaporation rate of the solvent and the in-depth consolidation of nanolimes. The addition of water to IP, which slows down the evaporation rate of the solvent, appears to have increased the penetration and degree of consolidation. However, this effect was not seen for the samples treated with ET and WET, where the addition of water to the ET solvent did not yield an increase in penetration and consolidation degree. This could be attributed to the fact that the nanolime used by Borsoi et. al. was synthesised by solvothermal reactions while the nanolime used in this work was prepared by an anion exchange process. Both types of nanolimes present slightly different properties such as colloidal stability, reactivity and morphology [12, 21] which could have affected their behaviour.

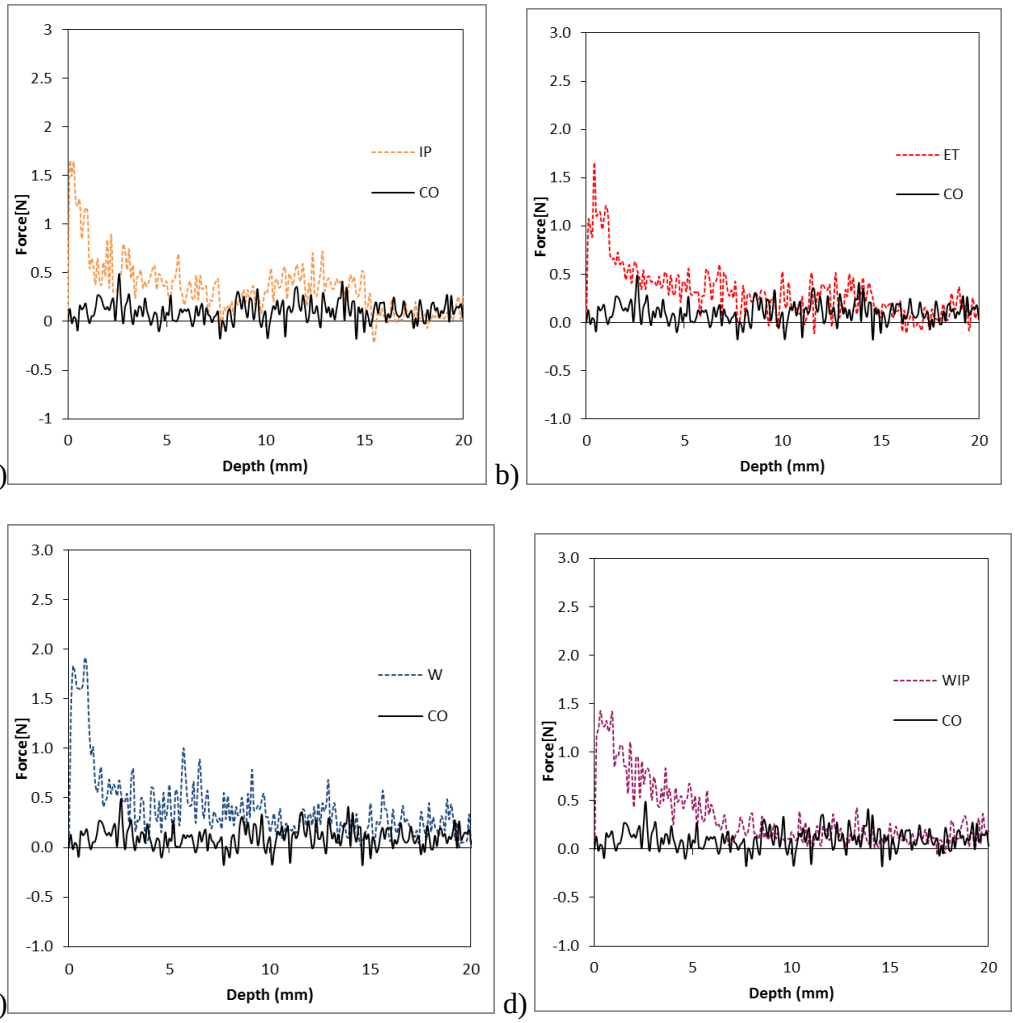

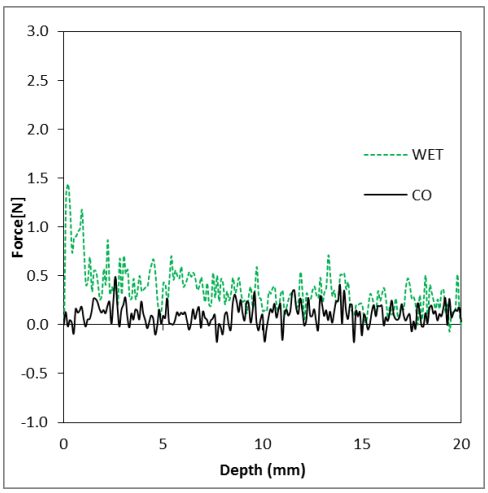

e)

Figure 10. Drilling resistance profiles for control and treated samples: a) IP; b) ET; c) W; d) WIP; and e) WET.

Comparing the SEM images of control (Fig. 11a) and treated surface samples (Fig. 11b-f) show how the new calcitic material fills the voids. These micrographs are in line with previous results of MIP and suggest a slight reduction of the porosity of the mortar surface which is confirmed by STT showing that the surface is significantly more compact after treatment as a result of the nanoline presence at the mortar's surface. The surface morphology was significantly altered after the application of the nanolime treatments. Fig 11 shows how all nanolime treatments covered the consolidated surface, which also modifies the aesthetic color of the substrates (see below paragraph, colorimetric analysis).

a) 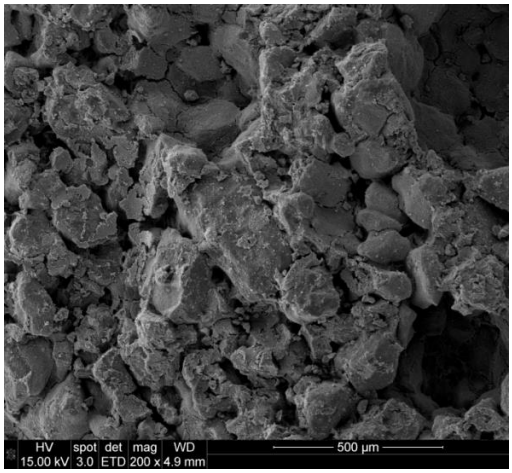

b) 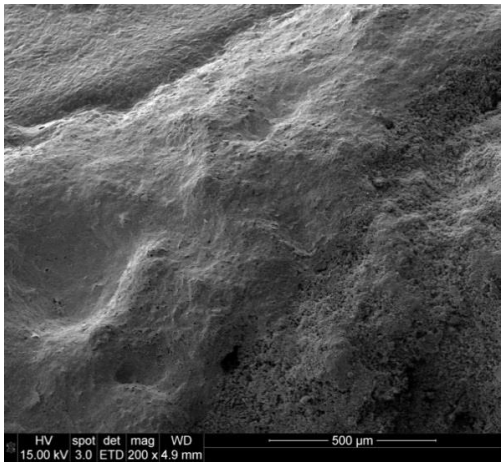

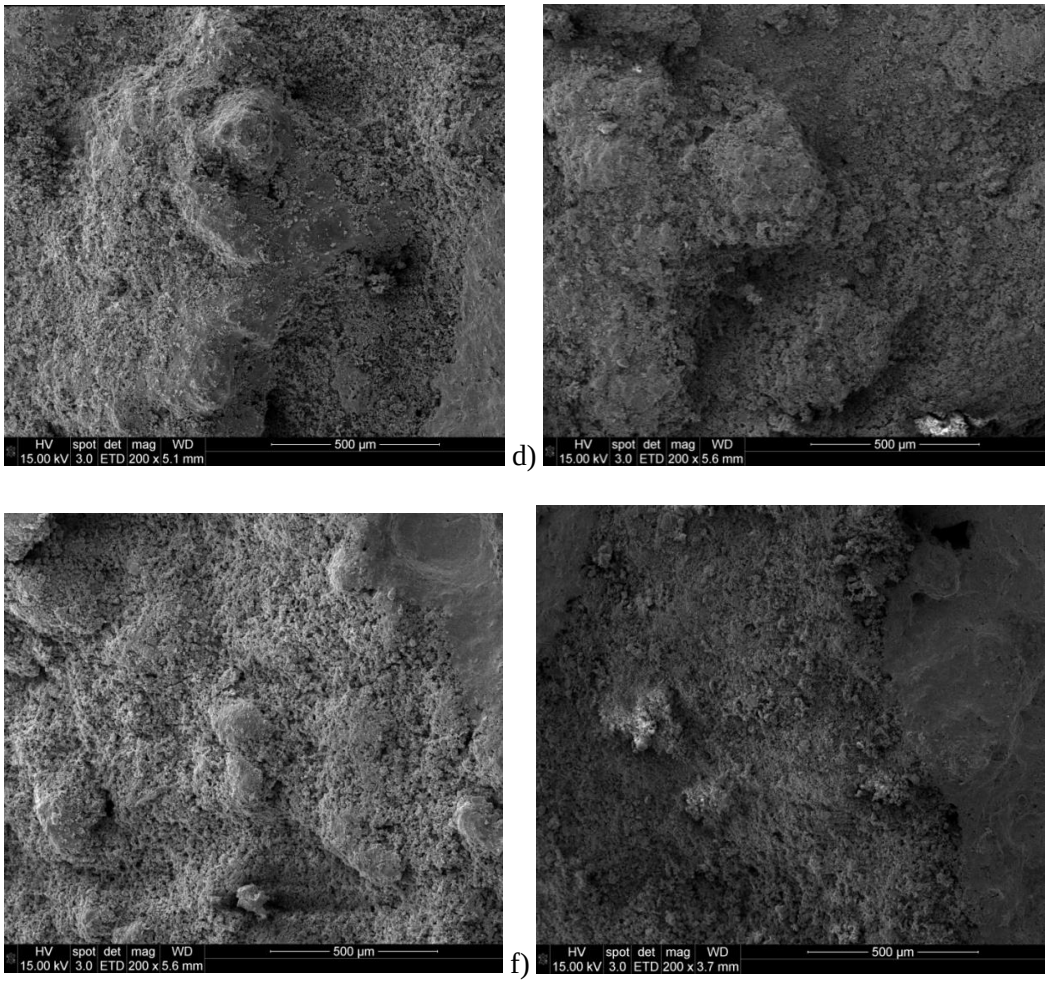

Figure 11. SEM micrographs of samples: a) control at 200x; b) IP sample at 200x; c) ET sample at 200x; d) W sample at 200x; e) WIP sample at 200x; f) WET sample at 200x.

A consolidation treatment should improve the physical-mechanical properties of a material a without changing its aesthetic appearance [43]. One of the most common nanolime side effects, which was already noticed in previous studies [12, 14; 32], is the whitening of the surface after treatment. Colorimetric results (Table 7) showed that all treatments, performed by brush, caused whitening of the specimens' surface above the ΔE=3 threshold. WIP obtained the lowest whitening and chromatic variations (ΔL* ~ 7 and ΔE* ~ 10 values) compared to the other treatments. This could be attributed to the higher colloidal stability of this suspension which facilitates its penetration deeper into the pores thus reducing particle accumulation on the surface. However, previous research had confirmed that the aesthetic alteration decreases after several wet-dry cycles without affecting the mechanical properties [12].

Table 7. Chromatic alterations resulting from the applied treatments. Mean values determined from 30 measurements

ΔL*	**Δa***	**Δb***	**ΔE***

IP	13.72 (±0.89)	-1.78 (±0.13)	-7.96 (±0.43)	15.96
ET	11.97 (±1.97)	-1.64 (±0.28)	-7.69 (±1.22)	14.32
W	11.92 (±1.87)	-1.65 (±0.31)	-8.12 (±1.13)	14.52
WIP	7.81 (±1.78)	-0.18 (±3.92)	-6.79 (±1.12)	10.35
WET	11.02 (±2.25)	5.33 (±1.60)	-7.78 (±1.05)	14.50

417

418

419 *4.2.4 Conclusions*

420 The present study has shown that $Ca(OH)_2$ nanoparticles synthesised by anion exchange process and dispersed in
421 various types of solvents can be effective as a consolidation treatment for porous lime mortars or other calcareous
422 building materials when applied by brushing. It has been shown that all treatments reduced the porosity of the
423 external part of the mortar. WIP and W seem to yield a slightly higher reduction of porosity followed by WET. The
424 porosity reduction in samples treated with WIP and WET can be attributed mainly to the reduction in the
425 population of pores with larger diameter size (17 to 100 μm) while IP and W seem to be more effective in filling
426 the pores with smaller size (0.05 to 0.7 μm).

427 The denser pore structure at the surface slightly affected the water absorption of the treated samples showing that
428 they slightly delayed the water absorption by capillarity compared to control samples. WIP and W seems to present
429 higher reduction of the water absorption by capillarity than the other treatments. This result appears to be in
430 accordance with the MIP results reported above which suggest that WIP and W treatments yielded higher reduction
431 of the porosity.

432 All treated samples presented similar drying rates to each other and all needed more time to dry than the control
433 due to the denser pore network on the mortars' surface. This is not desirable as it could increase the risk of several
434 decay processes (e.g. spalling from freeze-thaw or biological growth).

435 All nanolime treatments increased the drilling resistance of the superficial mortar layer. DRMS results showed that
436 IP, ET, W and WET treatments clearly increased the drilling resistance of the mortar within about 2-3 mm from the
437 surface. Additionally, a light consolidation effect was also noticeable up to 10 mm for these samples. In contrast,
438 the consolidation effect of WIP appears to be more homogeneous within a depth of 6-7 mm which might be
439 attributed to the slightly slower evaporation rate of the azeotropic mixture. W sample presented the highest increase
440 in the drilling resistance in the outer 2-3 mm (>1.5 N), together with a slight increase up to about 20 mm. This can
441 be attributed to the high reactivity of the nanoparticles and the low kinetic stability of this suspension, which could
442 facilitate the carbonation of the nanoparticles on the surface. However, more research must be carried out to fully

443 understand the penetration and consolidation mechanism of the nanolime suspensions. Furthermore, research is
444 needed to investigate the long-term performance of nanolime treatments focusing on possible weathering processes
445 such as freeze-thaw or salt crystallization.
446
447 All treatments produced whitening of the substrate's surface after application by brush. WIP treatment yielded the
448 lowest whitening and chromatic variations compared to the other treatments, which is slightly higher than the
449 thresholds generally accepted ($\Delta E>3$). The whitening effect associated with treatments decreased to values which
450 are imperceptible to the naked eye after exposing the samples to the accelerating weathering test [12]. However, in
451 order to fulfil the aesthetic compatibility requirements also in short times, a more in deep study of the application
452 procedure should be performed.
453
454 According to the above results, in the conditions here described, the WIP treatment seems to present slightly better
455 consolidating properties on the highly porous lime-mortars in terms of increased drilling resistance, higher
456 reduction of porosity, higher delay of the water absorption by capillarity, and lower impact on aesthetic properties
457 compared to the other suspensions. However, the data showed no drastic differences among the solvents, thus more
458 research seems to be necessary to fully understand the influence of solvent on the consolidation effectiveness.
459

460 **Acknowledgements**

461 This research has been funded by the Vice Chancellor's Scholarship within the Doctorate Program by Sheffield
462 Hallam University (UK). Authors want to thank Dr. Anthony Bell for his support with Rietveld refinements.
463

464 **References**

465 [1] Doehne E., Price C. A., (2010), "Stone Conservation: An Overview of Current Research", Research in
466 conservation Series, Getty Conservation Institute, USA.
467
468 [2] ICOMOS, (1964), "The Venice Charter", International Charter for the Conservation and Restoration of
469 Monuments and Sites.
470

[3] Wheeler G., (2005), "Alkoxysilanes and Consolidation of stone", Research in conservation Series, Getty Conservation Institute, USA

[4] Wheeler G., (2008), "Alkoxysilanes and the consolidation of stone: Where we are now. In Stone Consolidation in Cultural Heritage: Research and Practice", Proceedings of the International Symposium, Lisbon, 6-7 May 2008, ed. J. Delgado-Rodriguez and J. M. Mimoso, 41-52. Lisbon: LNEC (Laboratorio National de Engeneria Civil).

[5] Ferreira-Pinto, A. P. and Delgado-Rodrigues J., (2008), "Hydroxylating conversion treatment and alkoxysilane coupling agent as pre-treatment for the consolidation of limestones with ethyl silicate". In Stone Consolidation in Cultural Heritage: Research and Practice; Proceedings of the International Symposium, Lisbon, 6-7 May 2008, ed. J. Delgado-Rodriguez and J. M. Mimoso, 41-52. Lisbon: LNEC (Laboratorio National de Engenheria Civil).

[6] Pozo-Antonio, J.S., Otero.J, Alonso P., et al, (2019), Nanolime- and nanosilica-based consolidants applied on heated granite and limestone: Effectiveness and durability, Construction and Building Materials, 201, pp.852-870.

[7] Price, C., Ross, K., White, G., (1988), "A further appraisal of the 'Lime Technique' for limestone consolidation, using a radioactive tracer". IIC journal.Studies in Conservation, vol. 33 (4), pp.178–186.

[8] Clarke, B. L., and J. Ashurst, (1972), Stone Preservation Experiments. Watford: Building Research Establishment; London: Directorate of Ancient Monuments and Special Services.

[9] Sassoni, E., Naidu, S., Scherer, G.W., (2011), The use of hydroxyapatite as a new inorganic consolidant for damaged carbonate stones, Journal of Cultural Heritage, vol. 12, pp. 346–355.

[10] Natali, I., Tomasin, P., Becherini, F., Bernardi, A.,et al., (2015), Innovative consolidating products for stone materials: field exposure tests as a valid approach for assessing durability, vol. 3 (6), Heritage Science.

[11] Ambrosi, M., Dei L., Giorgi R., et al., (2001), "Colloidal particles of $Ca(OH)_2$: Properties and applications to restoration of frescoes", Langmuir, 17(14), pp.4251–4255.

[12] Otero J., Starinieri V., Charola A. E., (2018), "Nanolime for the consolidation of lime mortars: a comparison of three available products", Journal of Construction and Building Materials Vol. 181, pp.394-407.

[13] Rodriguez-Navarro C., Ruiz-Agudo E., (2017), "Nanolimes: from synthesis to application", Pure and Applied Chemistry, Volume 90, Issue 3, Pages 523–550, ISSN (Online) 1365-3075, ISSN (Print) 0033-4545, DOI: https://doi.org/10.1515/pac-2017-0506.

[14] Baglioni, P., Chelazzi D., Giorgi R., et al, (2014), "Commercial $Ca(OH)_2$ nanoparticles for the consolidation of immovable works of art". Applied physics. A, Materials science & Processing, 114(3), pp.723–732

[15] Sequeira, S., Casanova C., Cabrita E. J., (2006), "Deacidification of paper using dispersions of $Ca(OH)_2$ nanoparticles in isopropanol", Journal Cultural Heritage, 7, pp.264–272.

[16] Giorgi R., Dei L., Ceccato M., et al, (2002), "Nanotechnologies for Conservation of Cultural Heritage: Paper and Canvas Deacidification", Langmuir 18(21), pp.8198-8203. **DOI:** 10.1021/la025964d

[17] Natali I., Tempesti P., Carretti E., et al, (2014), "Aragonite Crystals Grown on Bones by Reaction of CO2 with Nanostructured $Ca(OH)_2$ in the Presence of Collagen. Implications in Archaeology and Paleontology", Langmuir 30(2), 660-668.

[18] Poggi, G., Toccafondi N., Chelazzi D., et al, (2016), "Calcium hydroxide nanoparticles from solvothermal reaction for the deacidification of degraded waterlogged wood". Journal of Colloid and Interface Science, 473, pp.1–8.

[19] Borsoi G., Tavares M., Veiga R., et al, (2012), "Microstructural characterization of consolidant products for historial renders: an innovative nanostructured lime dispersion and a more traditional ethyl silicate limewater solution", Journal of microscopy Society of America, 18(5), pp. 1181-9.

[20] Costa D., Delgado-Rodrigues J., (2012), "Consolidation of a porous limestone with nano-lime", in: G. Wheeler (Ed.), 12th International congress on the deterioration and conservation of stone, New York, pp. 10–19.

[21] Arizzi, A., Gomez-Villalba L. S., Lopez-Arce P., et al., (2015), "Lime mortar consolidation with nanostructured calcium hydroxide dispersions: the efficacy of different consolidating products for heritage conservation". European Journal of Mineralogy, 27(3), pp.311–323.

[22] Slizkova, Z., Dracky M., Viani A., (2015), "Consolidation of weak mortars by means of saturated solution of calcium hydroxide or barium hydroxide", Journal of Cultural Heritage, vol. 16, No. 4, pp. 420-460.

[23] López-Arce, P., Gomez-Villalba L.S., Pinho L., et al., (2010), "Influence of porosity and relative humidity on consolidation of dolostone with calcium hydroxide nanoparticles: Effectiveness assessment with non-destructive techniques". Materials Characterization, 61(2), pp.168–184.

[24] Taglieri, G., Felice, B., Daniele, V., Volpe, R., Mondelli C., (2016), "Analysis of the carbonatation process of nanosized $Ca(OH)_2$ particles synthesized by exchange ion process ". Proc Inst Mech Eng., 230, pp. 25-31.

[25] Dei, L., and Salvadori, B., (2006), "Nanotechnology in cultural heritage conservation: nanometric slaked lime saves architectonic and artistic surfaces from decay". Journal of Cultural Heritage, 7(2), pp.110–115.

[26] Daniele, V., Taglieri, G., (2010), "Nanolime suspensions applied on natural lithotypes: The influence of concentration and residual water content on carbonatation process and on treatment effectiveness". Journal of Cultural Heritage, 11(1), pp.102–106.

[27] Otero J., Starinieri V., Charola A. E., (2019), "Influence of substrate pore structure and nanolime particle size on the effectiveness of nanolime treatments", Journal of Construction and Building Materials 209, pp.701-708.

[28] Rodriguez-Navarro, C., Bettori I., Ruiz-Agudo E., (2016), "Kinetics and mechanism of calcium hydroxide conversion into calcium alkoxides: Implications in heritage conservation using nanolimes", Langmuir, 32(20), pp. 5183-5194.

[29] Borsoi, G., Lubelli B., Van Hees R. et al., (2016a), "Effect of solvent on nanolime transport within limestone: How to improve in-depth deposition". Colloids and Surfaces A: Physicochemical and Engineering Aspects, 497, pp.171–181.

[30] Borsoi, G., Lubelli, B., van Hees, R. et al. (2016b), "Optimization of nanolime solvent for the consolidation of coarse porous limestone", Appl. Phys. A (2016) 122: 846. https://doi.org/10.1007/s00339-016-0382-3

[31] Taglieri G, Daniele V., Macera L., Mondelli C., (2017), "Nano $Ca(OH)_2$ synthesis using a cost-effective and innovative method: Reactivity study", J Am Ceram Soc. 2017;100:5766–5778

[32] Taglieri G., Otero J., Daniele V., et. al., (2017), "The biocalcarenite stone of Agrigento (Italy): Preliminary investigations of compatible nanolime treatments", Journal of Cultural Heritage

[33] Daniele V., Taglieri G., Macera L., et al (2018), Green approach for an eco-compatible consolidation of the Agrigento biocalcarenites surface, Construction and Building Materials vol. 186, pp.1188-1199

[34] Borsoi G., Lubelli B., Van Hees R.P.J., et al, (2015), "Understanding the transport of nanolime consolidants within Maastricht limestone", Journal of Cultural Heritage, pp. 1296-2074. DOI: 10.1016/j.culher.2015.07.014

[35] EN 1015-3:1999, The European Standard, (1999), Methods of test for mortar for masonry. Determination of consistence of fresh mortar (by flow table).

[36] EN 1015-2:1998, The European Standard, (1998), Methods of test for mortar for masonry. Bulk sampling of

mortars and preparation of test mortars.

[37] Rietveld H.M., (1969), "A profile refinement method for nuclear and magnetic structures", Journal Applied Crystallography, 10, 65.

[38] Bish D. L. and Post J. E., (1989), Modern powder diffraction. Mineralogical Society of America, Crystal Reasearch & Technology, Washington. ISBN 0‐939950‐24‐3.

[39] Volpe R., Taglieri G., Daniele V., et. al., (2016), "A process for the synthesis of $Ca(OH)_2$ nanoparticles by means of ionic exchange resin", European patent EP2880101.

[40] Taglieri, G., Daniele V., Del Re G., Volpe, R., (2015), "A new and original method to produce $Ca(OH)_2$ nanoparticles by using an anion exchange resin". Advances in Nanoparticles, 4, pp.17–24.

[41] Taglieri, G., Daniele, V., Macera, L., (2019), Synthesizing alkaline earth metal hydroxides nanoparticles through an innovative single-step and eco-friendly method, Solid State Phenom., vol. 286, pp. 3–14.

[42] Otero J., Charola A. E., Grissom C. A., Starinieri V., (2017), "An overview of nanolime as a consolidation method for calcareous substrates", GE-Conservacion, 1 (11), 71-78pp.71-78

[43] Rodriguez-Navarro C., Suzuki A., Ruiz-Agudo E., (2013), "Alcohol dispersions of calcium hydroxide nanoparticles for stone conservation", Langmuir vol. 29, pp. 11457−11470.

[44] Otero J., Charola A. E., Starinieri V., (2019), Sticky rice–nanolime as a consolidation treatment for lime mortars, Journal of Material Science, Vol. 54, Issue 14, pp. 10217-10234.

[45] EN 16322. (2013), The European Standard CEN - Conservation of Cultural Heritage - Test methods - determination of drying properties.

[46] EN 13755, (2008), The English Standard for Natural stone test methods. Determination of water absorption at atmospheric pressure.

[47] ASTM C 67-00: Standard Test Methods for Measuring Apparent Porosity at atmospheric pressure, (2000), ASTM

[48] ASTM D3359-02: Standard Test Methods for Measuring Adhesion by Tape Test, (2002), ASTM International, 10 August.

[49] Charola A. E. and Wendler E., (2015), "An overview of the water-Porous building materials interactions", Restoration of Building and Monuments Journal, vol. 21(2-3), pp. 55-63.